Linking the North Atlantic Oscillation to winter precipitation over the Western Himalaya through disturbances of the subtropical jet

Kieran M R Hunt[1,2], Sumira Nazir Zaz[3], and Shakil Ahmed Romshoo[3]
[1]Department of Meteorology, University of Reading, United Kingdom
[2]National Centre for Atmospheric Science, University of Reading, United Kingdom
[3]Department of Geoinformatics, University of Kashmir, India

Corresponding author: Kieran M R Hunt (k.m.r.hunt@reading.ac.uk)

Key points

- Winter months where the NAO is significantly positive result in nearly 50% more precipitation over the Western Himalaya than when negative.
- This is caused by a more intense subtropical jet leading to more frequent (20%) and more intense (7%) winter storms over the region.
- This relationship between the NAO and winter storms is strongest on 2-3 and 12-16 year timescales.

Abstract

Winter (December to March) precipitation is vital to the agriculture and water security of the Western Himalaya and is largely brought to the region by extratropical systems, known as western disturbances (WDs), which are embedded in the subtropical jet. In this study, using seventy years of data, it is shown that during positive phases of the North Atlantic Oscillation (NAO+), the subtropical jet is significantly more intense than during negative phases (NAO-). Accordingly, the NAO affects WD behaviour on 2-3 year and 12-16 year timescales: during NAO+ periods, WDs are on average 20% more common and 7% more intense than during NAO- periods. This results in 40% more moisture flux entering the region and impinging on the Western Himalaya and an average increase in winter precipitation of 45% in NAO+ compared to NAO-.

Plain language summary

In this paper, we demonstrate a potential pathway for the North Atlantic Oscillation (NAO) to affect winter precipitation over the Western Himalaya. During positive phases of the NAO, the subtropical westerly jet – the jet stream that stretches across North Africa and South Asia – intensifies. Storms moving along the jet are both more common and more intense when the jet is stronger, due to greater shear and instability. As a result, positive phases of the NAO are associated with nearly 50% more winter precipitation over the Western Himalaya than negative phases. This result has significant implications for water security on seasonal timescales.

1. Introduction

The Western Himalaya and surrounding region receives most of its precipitation during the winter months (Dec–Mar) as the subtropical jet moves southwards, bringing extratropical storms known as western disturbances (WDs). WDs bring rainfall to lower elevations, where it is important for agriculture and snow to higher elevations, where it is important for replenishing glaciers and deepening the snowpack, both of which are subsequently vital for water security in the spring. Inconsistency in WD frequency and behaviour can thus affect the ecology, socioeconomics, health conditions of the Himalayan region and are often associated with hydro-meteorological disasters like floods, landslides and avalanches across the Himalaya and surrounding regions. Because WDs bring the majority of winter precipitation to the Western Himalaya (Midhuna et al., 2020), and because they are intimately linked with the behaviour of the subtropical jet (Hunt et al., 2018), there is the opportunity for seasonal predictability through global teleconnections that influence the position and intensity of the jet, such as the North Atlantic Oscillation (NAO) and ENSO. The NAO is a major mode of winter variability in the Northern Hemisphere, its effect extending from North America to Europe and a large portion of Asia (Hurrell et al., 2003) and accounts for more than 36% of the variance in mean sea level pressure during winter months (Walker and Bliss 1932).

The statistical relationship between the NAO and winter precipitation over the western Himalaya has been explored previously, but authors have disagreed on both the sign and significance of the relationship. Using a 21-year rolling window, Yadav et al. (2009) showed that the NAO is positively correlated with winter precipitation over northwest India, and that this relationship was

strongest between 1940 and 1980 (when the mean correlation coefficient was 0.42). Using composite analysis, they showed that positive phases of the NAO during this period resulted in a stronger meridional pressure gradient over Europe and North Africa, resulting in a stronger subtropical jet, and hence, they hypothesised, more intense WDs – a result later corroborated by Attada et al. (2019). They noted a weakening of this relationship over recent decades in favour of a strengthening relationship with ENSO. A similar analysis by Nageswararao et al (2016) also found a positive correlation between NAO and winter precipitation over North India that peaked in the 1960s. Zaz et al. (2018) found a strong positive correlation (0.68) between the NAO and seasonal mean winter precipitation over Jammu and Kashmir, which they attributed to local meridional displacement of the subtropical westerly jet. Like Nageswararao et al (2016), they highlighted an increasing influence of the Arctic Oscillation over recent decades.

Other studies have found a positive correlation through more indirect means. Nageswararao et al. (2018) showed that wheat production (typically grown in the winter months) in northwest India was strongly correlated with NAO and AO activity. Forke et al. (2019) analysed carbonate sediments in the Arabian Sea and found that increased winter runoff was associated with periods of positive ENSO and positive NAO. Greene and Robertson (2017) found evidence of a link between the NAO and decadal variability of winter and spring precipitation in the Upper Indus Basin in CMIP5 models. Hingmire et al. (2019) found that non-foggy days over the Indo-Gangetic Plain – which they associated with the presence of WDs – preferentially occurred during periods of positive NAO, although this result may be complicated by the fact that WDs often are associated with fog (e.g., Sawaisarje et al., 2014; Patil et al., 2020). Syed et al. (2010) used a regional climate model to investigate the effects of the NAO and ENSO on precipitation over North Pakistan, Afghanistan and Tajikistan and found that positive phases of the NAO were associated with anomalously low 500 hPa height over the region and associated moisture intake from Mediterranean, Caspian and Arabian Sea, leading to excess precipitation.

In contrast, some studies have also asserted a negative correlation between the NAO and winter precipitation over the western Himalaya. Devi et al. (2020) constructed a simple seasonal forecast model to predict winter precipitation over the Western Himalaya and found a strong negative correlation with the NAO (-0.57). Basu et al (2017) attributed a weak 2015 winter monsoon to reduced WD activity as a result of positive ENSO and positive NAO, stating that the positive NAO set up an unfavourable standing wave in the subtropical jet with a blocking anticyclonic anomaly over the subcontinent. Using plankton-based proxies, Munz et al. (2017) showed that intense winter monsoons since 1750 coincided with strong negative phases of the NAO. Similarly, Giosan et al. (2018) used plankton-based proxies to show that strong winter monsoons during the mid-Holocene (4500 to 3000 years ago) were contemporaneous with a more negative NAO and southward migration of the subtropical jet, bringing increased WD activity to South Asia.

Not only do these studies disagree on the sign and significance of the relationship, but they are mostly statistical in nature. Our study proposes to resolve this by establishing causality between the NAO and downstream winter precipitation over the Western Himalaya, through the medium of WDs. We start by showing how the subtropical jet is affected by different NAO phases, then use wavelet analysis to link this relationship to WD behaviour. Finally, we use composite

analysis to show how this projects onto WD behaviour, moisture flux, and finally precipitation. The results of this study may help improve seasonal forecasts for WD-related winter precipitation which will in turn help in developing policies and mitigation strategies related to socio-economic and natural hazards associated with these disturbances.

2. Data

2.1 ERA5

To quantify moisture transport and the synoptic-scale structure of the troposphere over the Western Himalaya, we use data from the ECMWF ERA5 reanalysis (Hersbach et al., 2020). Data are available globally, at hourly resolution from 1950 onwards, on a 0.25°×0.25° grid. Data are available over 37 pressure levels from 1000 to 0.01 hPa, as well as at selected heights above the surface. Data are assimilated into the forecasting system from a large variety of sources, including satellites, automatic weather stations, and radiosondes.

2.2 APHRODITE

Precipitation data in this study come from the APHRODITE-2 project (Yatagai et al., 2012; Yatagai et al., 2017) which is based on a dense network of in-situ gauge data, gridded using a kriging method to 0.25°×0.25° at daily resolution. The dataset runs from 1951 to 2015. Over India, the rainfall amount recorded for a given day is the accumulation from 0300 UTC (0830 LT) the previous day through 0300 UTC of the current day. This dataset was chosen for its longevity and resolution. Given we are not interested in rainfall over the ocean, satellite data were not needed. Despite the relatively sparse gauge network over the Himalaya and Hindu Kush, APHRODITE was shown to outperform other datasets, including reanalyses and satellite products in this area (Baudouin et al., 2020).

2.3 Western disturbance database

For WD track and intensity information, we use the University of Reading ERA5-T42 track database, computed by applying the algorithm developed in Hunt et al. (2018). The mean relative vorticity in the 450-300 hPa is computed, and then spectrally truncated at T42 to remove small-scale features and other short-wavelength noise. Regions of positive vorticity are then identified, and their centroids linked subject to a set of physical constraints. The database is then filtered, removing tracks which do not pass-through north India (20°N–36.5°N, 60°E–80°E), last less than 48 hours, or dissipate at a point westward of their genesis. These data can be downloaded from http://gws-access.jasmin.ac.uk/ public/incompass/kieran/iiser/.

2.4 NAO Index

For NAO data, we use the monthly index published by the NWS CPC, available from 1950 onwards. The index is computed by applying a rotated principal component analysis (Barnston and Livezey, 1987) to standardised 500 hPa geopotential height anomalies between 20° and 90°N. The NAO has highest variance in the winter months. Throughout, we define NAO+ as months where the NAO index is greater than 1 (giving 160 months in total, 49 in winter), and NAO- as months where the index is less than -1 (giving 142 months in total, 58 in winter). Data

can be downloaded from https://www.cpc.ncep.noaa.gov/products/precip/CWlink/pna/nao.shtml.

2.5 Wavelet spectra

Wavelet power spectra are computed using the PyCWT library (https://pycwt.readthedocs.io/), which is based on Torrence and Compo (1998). For our wavelet analysis, we use a derivative-of-Gaussian continuous wavelet. This only has a real part, and thus computed power identifies the individual peaks and troughs of the underlying data.

3. Results

It is known that the NAO can substantially affect the location and intensity of the North Atlantic jet stream (Woolings and Blackburn, 2012). As the North Atlantic jet and the subtropical westerly jet (SWJ) over Eurasia are linked (Strong and Davis, 2008), this provides a potential physical pathway between the NAO and the Western Himalaya. Figure 1 shows the climatology of global subtropical jets during winter months and how that climatology changes during NAO+ and NAO- months.

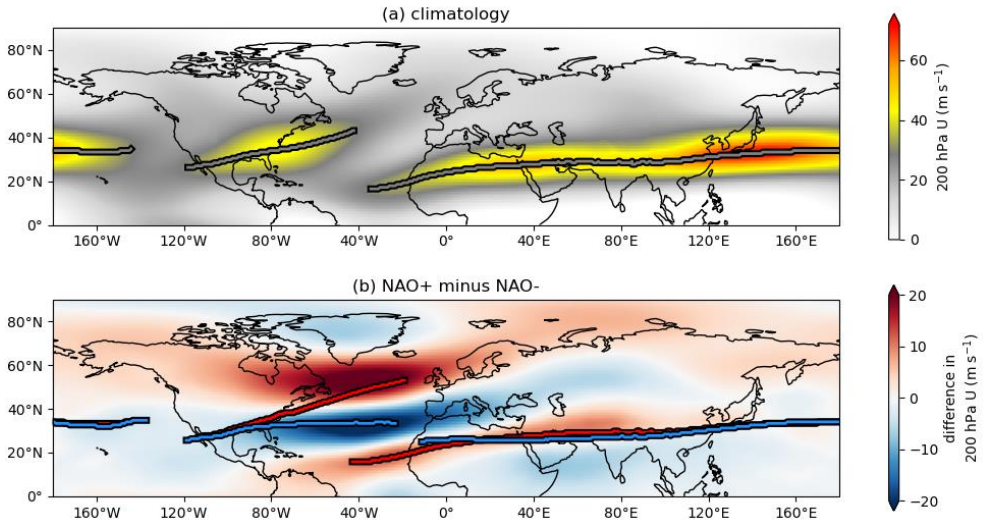

Figure 1. Zonal wind speed at 200 hPa and location of the Northern Hemisphere westerly jet axis for (a) the Dec–Mar climatology and (b) the difference between NAO+ and NAO-. The jet axis is defined as a meridional local maximum in 200 hPa U wherever U >30 m s^{-1}. In (b) the jet axes are shown for both composite NAO+ (red) and NAO- (blue).

The climatological subtropical jet has two distinct branches: a short one over North America and the North Atlantic, closely associated with North Atlantic storm tracks, and a longer one covering North Africa and South Asia, in which WDs are embedded. During NAO+ months, the North Atlantic jet moves northwards, responding to the strong meridional pressure gradient there. During NAO- months, the North Atlantic jet moves southward, almost merging with the subtropical jet over Africa. Despite this, the subtropical jet is more intense and less stable during NAO+, likely owing to an increased upper-level meridional temperature gradient in the midlatitudes and stronger eddy forcing (e.g., Li et al., 2021). There is also a slight meridional

shift in the jet axis as it passes over India, where it is about 200 km further north during NAO+ than NAO-.

It is known that both the latitude of the subtropical jet (Hunt et al., 2017) and its intensity (Hunt et al. 2018) exert controls on WD behaviour over South Asia. In addition, the greater vertical wind shear exerted by a stronger jet is associated with more intense updrafts in WDs (Baudouin et al., 2021). As the NAO affects both of these jet characteristics, we can reasonably hypothesise that it will also modulate downstream WD behaviour. We test this hypothesis in two ways, using both wavelet and compositing techniques. Figure 2 shows the frequency spectra for both the NAO index (a,b) and WD frequency (c,d) between 1950 and 2020, computed using a derivative-of-Gaussian wavelet. Because this wavelet only has a real part, the spectra highlight the locations of peaks and troughs (both have high power) across the range of frequencies. Black contours that mark the locations of significant peaks and troughs of the NAO are superimposed on the WD frequency spectrum so that potential regions of overlap can be identified.

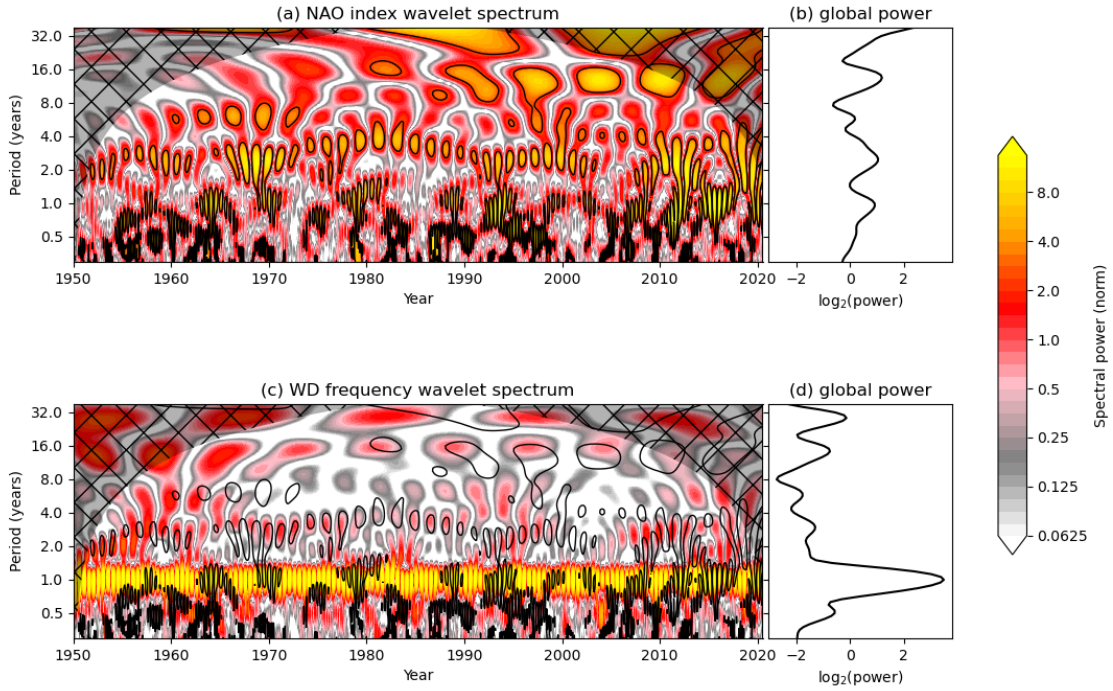

Figure 2. Frequency spectra of (a,b) the NAO and (c,d) WD frequency over South Asia, computed using a derivative of Gaussian wavelet with an angular frequency of one month. Both the NAO index and WD frequency are standardised before computation, so that the spectral power is normed. Black line contours on the power spectra (a,c) indicate where the NAO spectral power is significantly greater than zero at a 90% confidence level. Hatching on the power spectra (a,c) indicates the cone of influence, where edge effects are significant.

Spectral power in the NAO index is largely concentrated into three bands: annual, 2-3 year, and 12-16 year. The sub-annual bands also contain some periods of significantly high power, and there may be power at much lower frequencies not detectable in the 70-year dataset used here (e.g. Trouet et al., 2009). The WD frequency spectrum is dominated by annual variability; this is expected since WDs are almost entirely absent during the summer monsoon (June to

September) but occur at rates approaching ten per month during the winter. This annual cycle is also controlled by the subtropical jet, which migrates northward over China every summer in response to seasonal shifts in the Hadley Cell (Schiemann et al., 2009) and is not related to the NAO.

The two other bandwidths with significant NAO activity, 2-3 year and 12-16 year, show evidence of relationship with WD frequency. Peaks and troughs within the 2-3 year band align closely with those in the WD frequency spectrum, especially between 1950 and 2000 and most strongly between 1970 and 1990, which may partially explain why previous authors have noted declining correlations between the NAO and synoptic winter activity over the Western Himalaya since the 1980s. Interestingly, there are two periods where NAO power in this band weakens significantly, 1963–66 and 2003–7, during which the WD frequency power in this band also weakens significantly. There is a slowly varying lag relationship between the two: sometimes the extrema coincide, whereas sometimes the extrema in the NAO spectrum lead the extrema in the WD spectrum by as much as six months. Since 1980, there has also been a marked overlap in the extrema of the 12-16 year band of both datasets, although the relationship is weaker here than in the 2-3 year band. These results lend credibility to the idea that the NAO can modulate WD frequency through its interactions with the subtropical jet.

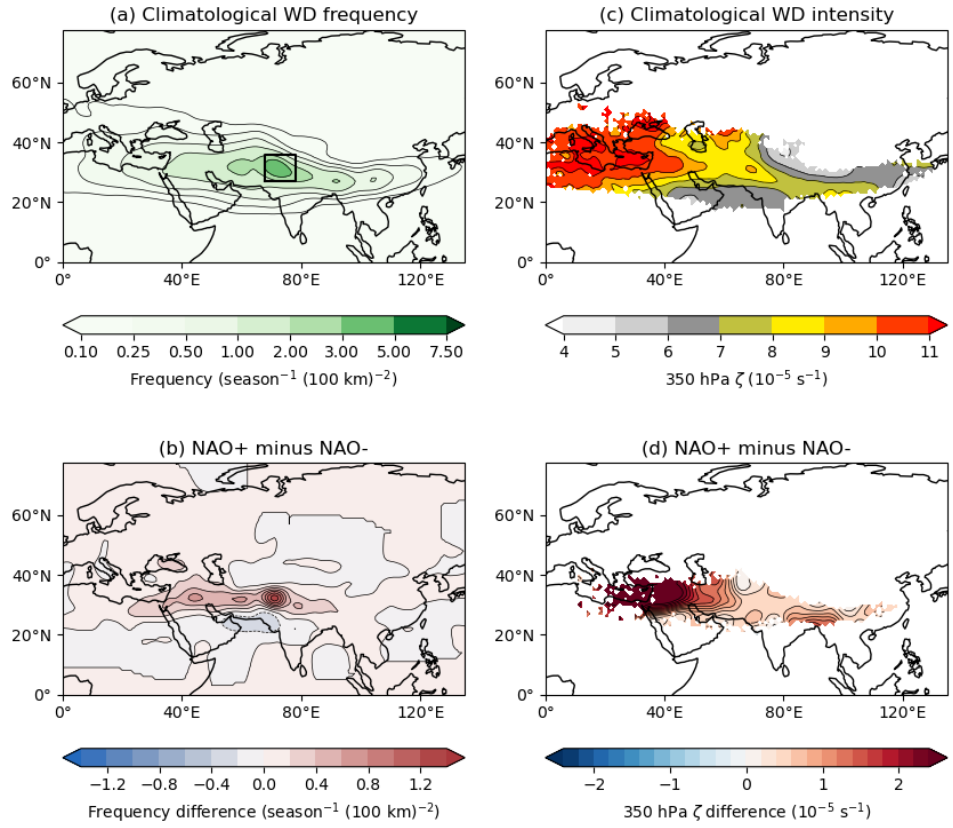

Figure 3. The role of the NAO in modulating WD frequency and intensity. (a) climatological frequency in Dec–Mar; (b) composite difference in frequency between NAO+ and NAO- months; (c) climatological intensity in Dec–Mar; and (d) composite difference in intensity between NAO+ and NAO- months. The region with the highest climatological winter precipitation and WD frequency surrounding the Western Himalaya is marked with a black rectangle in (a).

To explore this relationship further, we composite spatial maps of WD frequency and intensity and contrast them between NAO+ and NAO- periods. Although this method does not capture lead-lag relationships between the two, their extrema are sufficiently simultaneous that this should not be a problem. These composites are shown in Figure 3. The highest values of WD frequency are found over the Western Himalaya, where the maximum value is about 4.3 season^{-1} (100 km)$^{-2}$. Over the box [68-78°E, 27-38°N; marked in Figures 3 and 4] which contains the Western Himalaya, the highest climatological WD frequency, and the highest mean winter precipitation, the mean WD frequency is about 2.6 season^{-1} (100 km)$^{-2}$. During NAO+, the peak value is 31% higher than during NAO- (Fig. 3b), and the average frequency over the box is 20% higher. Following the slight northward shift in the subtropical jet during NAO+ (see Figure 1), there is a marginal poleward shift in the location of highest WD frequency. There is also a significant change to the mean intensity: the average 350 hPa relative vorticity at the centre of WDs passing through the box is 7.7×10^{-5} s^{-1}; this is 7% higher during NAO+ than NAO-.

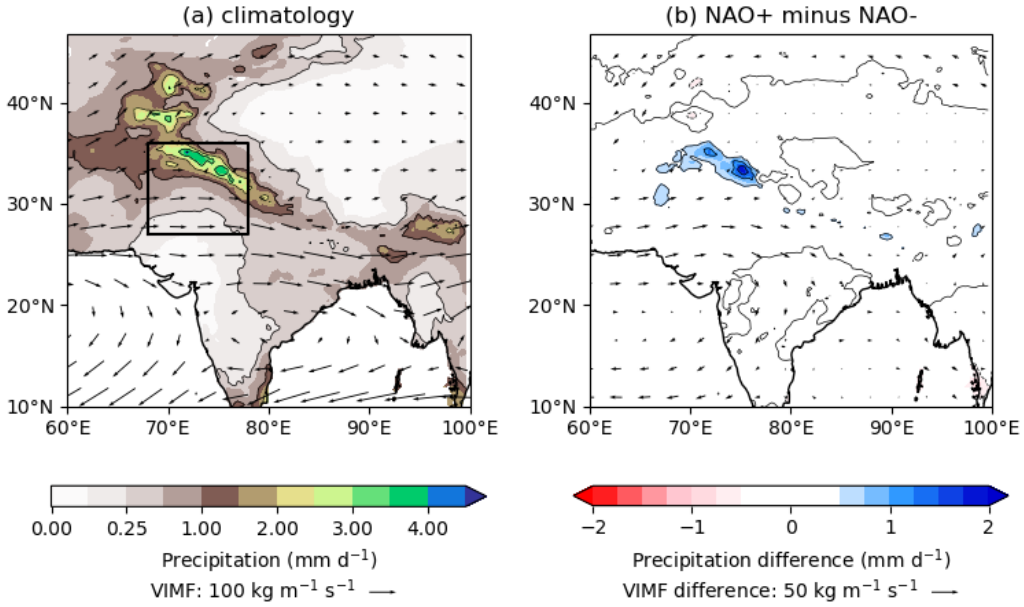

Figure 4. Effect of the NAO on Dec–Mar precipitation and vertically integrated moisture flux convergence over South Asia. (a) Dec–Mar climatology and (b) composite difference between NAO+ and NAO- months. The black rectangle in (a) marks the same region as in Figure 3.

Both WD frequency and intensity exert strong controls on precipitation over the Western Himalaya and surrounding region by modulating southwesterly moisture flux from the Arabian Sea. Figure 4 shows the climatology of winter precipitation and vertically-integrated moisture flux over South Asia and how these fields change between NAO+ and NAO-. Mean precipitation within the black rectangle over the APHRODITE period (1950–2015) is 0.97 mm d^{-1} with a peak value of 4.22 mm d^{-1}. During NAO+, these are 45% and 57% higher respectively than in NAO-. Much of this change can be explained by increased moisture flux entering the box and impinging on the orography. The mean value is 47.8 kg m^{-1} s^{-1}, which is 39.9% larger during NAO+ than NAO-.

4. Conclusions

Winter (Dec–Mar) precipitation is vital to the Western Himalaya and surrounding region. At low elevation, it provides the rainfall needed to grow rabi crops; at higher elevations, it provides snowfall, which, when it melts later in the year, is a crucial component of the region's water security. As such, identifying potential sources of predictability for seasonal and subseasonal precipitation is important for improving both preparation and mitigation. Many previous studies have established a statistical relationship between Western Himalaya winter precipitation and the NAO, but these disagree on the significance, duration, and even sign of the relationship, with none establishing a causal mechanism.

In this study, we have used seventy years of reanalysis, precipitation and NAO data to confirm that there is a strong positive correlation between the NAO and winter precipitation over the Western Himalaya, and to demonstrate the mechanism through which this relationship is realised. In months where the NAO index is greater than 1 (NAO+), the subtropical jet is significantly more intense than in months where the NAO index is less than -1 (NAO-), likely as a result of a stronger upper-level meridional temperature gradient and greater eddy forcing upstream. This results in the production of more western disturbances (WDs), the winter storms that bring the majority of winter precipitation to the Western Himalaya. On average, WDs striking the Himalaya are 20% more common during NAO+ than during NAO-, rising to 31% in areas where WDs are most frequent. The more intense subtropical jet is also associated with an environment of greater baroclinic instability, meaning that WDs are about 7% more intense during NAO+ than during NAO-. Combined, these increases in WD frequency and intensity result in 40% moisture entering the region around the Western Himalaya, resulting in 45% more winter precipitation during NAO+ than during NAO-. Using wavelet analysis, we showed that the NAO modulates WD frequency most strongly on timescales of 2-3 years, with an additional contribution from the lower frequency 12-16 year band.

Further work is needed to address the precise set of mechanisms by which the NAO modulates the subtropical jet, to assess why the lag between the NAO and Western Himalaya precipitation varies between zero and six months, and to quantify the impact of the NAO on extreme precipitation events in the region. Future research may also want to explore the relationship between the NAO and the northeast monsoon over Sri Lanka and the southern states of India.

Data availability statement

All data used in this study were open access, with details on where to obtain them given in Section 2. No new datasets were produced as part of this study.

Acknowledgements

KMRH is funded through the Weather and Climate Science for Service Partnership (WCSSP) India, a collaborative initiative between the Met Office, supported by the UK Government's Newton Fund, and the Indian Ministry of Earth Sciences (MoES).

References

Attada, R., Dasari, H. P., Chowdary, J. S., &Yadav, R. K.. (2018). Surface air temperature variability over the Arabian Peninsula and its links to circulation patterns. *International Journal of Climatology.* 39(1), 445-464. doi:10.1002/joc.5821

Barnston, G.A., & Livezey, R. E. (1987). Classification, Seasonality and Persistence of Low-Frequency Atmospheric Circulation Patterns. *Monthly Weather Review*.115, 1083-1126. doi:10.1175/1520-0493 (1987)115<1083:CSAPOL>2.0.CO;2

Basu, S., Bieniek, P. A., & Deoras, A.,(2017) An investigation of reduced western disturbance activity over Northwest India in November - December 2015 compared to 2014 - A case study. *Asia-Pacific Journal of Atmospheric Sciences* 53(1) 75-83. doi:10.1007/s13143-017-0006-7

Baudouin, J. P., Herzog, M., & Petrie, C. A. (2020). Cross-validating precipitation datasets in the Indus River basin. *Hydrology and Earth System Sciences*, *24*(1), 427-450. doi:10.5194/hess-24-427-2020.

Baudouin, J-P., Herzog, M., & Petrie, C. A. (2021). Synoptic processes of winter precipitation in the Upper Indus Basin. *Weather and Climate Discussion*. In review. doi:10.5194/wcd-2021-45

Devi, U., Shekhar, M. S., Singh, G. P., & Dash, S. K. (2020). Statistical method of forecasting of seasonal precipitation over the Northwest Himalayas: North Atlantic Oscillation as precursor. *Pure and Applied Geophysics*, 1-11. doi:10.1007/s00024-019-02409-8

Forke, S., Rixen, T., Burdanowitz, N., Lückge, A., Ramaswamy, V., Munz, P., ... & Gaye, B. (2019). Sources of laminated sediments in the northeastern Arabian Sea off Pakistan and implications for sediment transport mechanisms during the late Holocene. *The Holocene*, *29*(1), 130-144. doi:10.1177/095968361880462

Greene, M, Arthur., Robertson A, W. (2017). Interannual and low-frequency variability of Upper Indus Basin winter/spring precipitation in observations and CMIP5 models. *Climate Dynamics*. 49, (11-12), 4171-4188 doi:10.1007/s00382-017-3571-7

Giosan, L., Orsi, W. D., Coolen, M., Wuchter, C., Dunlea, A. G., Thirumalai, K., ... & Fuller, D. Q. (2018). Neoglacial climate anomalies and the Harappan metamorphosis. *Climate of the Past*, 14(11), 1669-1686. doi:10.5194/cp-14-1669-2018

Hersbach, H., Bell, B., Berrisford, P., Hirahara, S., Horányi, A., Muñoz-Sabater, J., Nicolas, J., Peubey, C., Radu, R., Schepers, D. & Simmons, A. (2020). The ERA5 global reanalysis. *Quarterly Journal of the Royal Meteorological Society*, 146(730), 1999-2049. doi:10.1002/qj.3803.

Hingmire, D., Vellore, R. K., Krishnan, R., Ashtikar, N. V., Singh, B. B., Sabade, S., & Madhura, R. K. (2019). Widespread fog over the Indo-Gangetic Plains and possible links to

boreal winter teleconnections. *Climate Dynamics*, *52*(9), 5477-5506. doi:10.1007/s00382-018-4458-y

Hunt, K. M. R., Turner, A. G., & Shaffrey, L. C. (2017). The evolution, seasonality, and impacts of Western disturbances. *Quarterly Journal of the Royal Meteorological Society,* 144(710), 278–290. doi:10.1002/qj.3200

Hunt, K. M. R., Curio, J., Turner, A. G., & Schiemann, R. K. H. (2018). Subtropical westerly jet influence on occurrence of western disturbances and Tibetan Plateau vortices. *Geophysical Research Letters*, 45(16), 8629-8636. doi:10.1029/2018GL077734

Hunt, K. M. R., & Dimri, A. P. (2021). Synoptic-scale precursors of landslides in the western Himalaya and Karakoram. *Science of the Total Environment*, *776*, 145895. doi:10.1016/j.scitotenv.2021.145895

Hurrell, J. W. (2003). An overview of the North Atlantic Oscillation. In, Hurrell, JW, Y. Kushnir, G. Ottersen, and M. Visbeck. *The North Atlantic Oscillation: Climatic Significance and Environmental Impact*, 1-35. doi:10.1029/134GM01

Li, J., Li, F., He, S., Wang, H., & Orsolini, Y. J. (2021). The Atlantic Multidecadal Variability Phase Dependence of Teleconnection between the North Atlantic Oscillation in February and the Tibetan Plateau in March. *Journal of Climate*, *34*(11), 4227-4242. doi:10.1175/JCLI-D-20-0157.1

Midhuna, T. M., Kumar, P., & Dimri, A. P. (2020). A new western disturbance index for the Indian winter monsoon. *Journal of Earth System Science*, *129*(1), 1-14. doi:10.1007/s12040-019-1324-1

Munz, P. M., Lückge, A., Siccha, M., Böll, A., Forke, S., Kucera, M., & Schulz, H. (2017). The Indian winter monsoon and its response to external forcing over the last two and a half centuries. *Climate Dynamics*, *49*(5), 1801-1812. doi:10.1007/s00382-016-3403-1

Nageswararao, M. M., Mohanty, U. C., Ramakrishna, S. S. V. S., Nair, A., & Prasad, S. K. (2016). Characteristics of winter precipitation over Northwest India using high-resolution gridded dataset (1901–2013). *Global and Planetary Change*, *147*, 67-85. doi:10.1016/j.gloplacha.2016.10.017.

Nageswararao, M. M., Dhekale, B. S., & Mohanty, U. C. (2018). Impact of climate variability on various Rabi crops over Northwest India. *Theoretical and applied climatology*, *131*(1), 503-521. doi:10.1007/s00704-016-1991-7

Patil, M. N., Dharmaraj, T., Waghmare, R. T., Singh, S., Pithani, P., Kulkarni, R., ... & Ghude, S. (2020). Observations of carbon dioxide and turbulent fluxes during fog conditions in north India. *Journal of Earth System Science*, *129*(1), 1-12. doi:10.1007/s12040-019-1320-5

Sawaisarje, G. K., Khare, P., Shirke, C. V., Deepakumar, S. & Narkhede, N. M. (2014). Study of winter fog over Indian subcontinent: climatological perspectives. *Mausam*, 65(1), 19–28.

Schiemann, R., Lüthi, D., & Schär, C. (2009). Seasonality and interannual variability of the westerly jet in the Tibetan Plateau region. *Journal of climate*, *22*(11), 2940-2957. doi:10.1175/2008JCLI2625.1.

Strong, C., & R, E, Davis. (2008). Variability in the position and strength of winter jet stream cores related to Northern Hemisphere teleconnections. *Journal of Climate*. 21. 584–592. doi:10.1175/2007JCLI1723.1

Syed, F. S., Giorgi, F., Pal, J. S., & Keay, K. (2010). Regional climate model simulation of winter climate over Central–Southwest Asia, with emphasis on NAO and ENSO effects. *International Journal of Climatology: A Journal of the Royal Meteorological Society*, *30*(2), 220-235. doi:10.1002/joc.1887

Trouet, V., Esper, J., Graham, N. E., Baker, A., Scourse, J. D., & Frank, D. C. (2009). Persistent positive North Atlantic Oscillation mode dominated the medieval climate anomaly. *science*, *324*(5923), 78-80. doi:10.1126/science.1166349

Syed, F. S., Giorgi, F., Pal, J. S., & Keay, K. (2010). Regional climate model simulation of winter climate over Central–Southwest Asia, with emphasis on NAO and ENSO effects. *International Journal of Climatology: A Journal of the Royal Meteorological Society*, *30*(2), 220-235. doi:10.1002/joc.1887

Torrence, C., & Compo, G. P. (1998). A practical guide to wavelet analysis. *Bulletin of the American Meteorological society*, *79*(1), 61-78. doi:10.1175/1520-0477(1998)079<0061:APGTWA>2.0.CO;2

Walker, G. T., and E. W. Bliss. "Memoirs of the royal meteorological society." *World Weather V* 4 (1932): 53-84.

Woollings, T., & Blackburn, M. (2012). The North Atlantic jet stream under climate change and its relation to the NAO and EA patterns. *Journal of Climate*, *25*(3), 886-902. doi:10.1175/JCLI-D-11-00087.

Yadav, R. K., Rupa Kumar, K., & Rajeevan, M. (2009). Increasing influence of ENSO and decreasing influence of AO/NAO in the recent decades over northwest India winter precipitation. *Journal of Geophysical Research: Atmospheres*, *114*(D12). doi:10.1029/2008JD011318

Yatagai, A., Kamiguchi, K., Arakawa, O., Hamada, A., Yasutomi, N., & Kitoh, A. (2012). APHRODITE: Constructing a long-term daily gridded precipitation dataset for Asia based on a

dense network of rain gauges. *Bulletin of the American Meteorological Society*, *93*(9), 1401-1415. doi:10.1175/BAMS-D-11-00122.1

Yatagai, A., Masuda, N., Tanaka, K., & Higuchi, A. (2017). APHRODITE-2: Improved grid precipitation algorithm -- Initial results. *Abstracts of the Society of Hydrology and Water Resources*. 30. In Japanese.

Zaz, S. N., Romshoo, S. A., Ramkumar, T. K., & Babu, V. (2018). Climatic and extreme weather variations over mountainous Jammu and Kashmir, India: physical explanations based on observations and modelling. *Atmos Chem Phys Discuss.* 19, 15-37. doi:10.5194/acp-19-15-2019